

Electrochemistry Combined with LC–HRMS: Elucidating Transformation Products of the Recalcitrant Pharmaceutical Compound Carbamazepine Generated by the White-Rot Fungus *Pleurotus ostreatus*

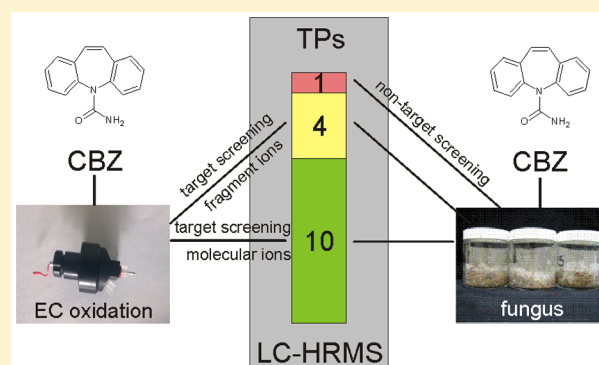
Bettina Seiwert,[†] Naama Golan-Rozen,[‡] Cindy Weidauer,[†] Christina Riemenschneider,[†] Benny Chefetz,[‡] Yitzhak Hadar,[‡] and Thorsten Reemtsma^{*,†}

[†]Department of Analytical Chemistry, Helmholtz Centre for Environmental Research–UFZ, Permoserstrasse 15, Leipzig 04318, Germany

[‡]Faculty of Agriculture, Food and Environment, The Hebrew University of Jerusalem, P.O. Box 12, Rehovot 76100, Israel

S Supporting Information

ABSTRACT: Transformation products (TPs) of environmental pollutants must be identified to understand biodegradation processes and reaction mechanisms and to assess the efficiency of treatment processes. The combination of oxidation by an electrochemical cell (EC) with analysis by liquid chromatography–high-resolution mass spectrometry (LC–HRMS) is a rapid approach for the determination and identification of TPs generated by natural microbial processes. Electrochemically generated TPs of the recalcitrant pharmaceutical carbamazepine (CBZ) were used for a target screening for TPs formed by the white-rot fungus *Pleurotus ostreatus*. EC with LC–HRMS facilitates detection and identification of TPs because the product spectrum is not superimposed with biogenic metabolites and elevated substrate concentrations can be used. A group of 10 TPs formed in the microbial process were detected by target screening for molecular ions, and another 4 were detected by screening on the basis of characteristic fragment ions. Three of these TPs have never been reported before. For CBZ, EC with LC–HRMS was found to be more effective than software tools in defining targets for the screening and faster than nontarget screening alone in TP identification. EC with LC–HRMS may be used to feed MS databases with spectra of possible TPs of larger numbers of environmental contaminants for an efficient target screening.



INTRODUCTION

Identification of transformation products (TPs) of environmental contaminants formed by living organisms is crucial to improving our understanding of biodegradation processes and better assessing contaminant fate in the environment and biota. Knowledge of TPs is also essential for assessing their toxicity. Because biologically generated TPs tend to be more polar than their parent compound, much of the work on TP identification relies on liquid chromatography coupled to mass spectrometry (LC–MS). Today, high-resolution (HR) MS is becoming popular because of its high selectivity and high mass accuracy, mostly in the form of Orbitrap or QqTOF mass spectrometers.¹

There are two obstacles to analyzing unknown TPs from complex biological samples: (a) determination of the chromatographic signals that correspond to TPs of the contaminant under study and (b) the (tentative) identification of these TPs, i.e., the determination of their molecular formula from the exact mass of the molecular ions or their adducts and structure

elucidation on the basis of the product ion spectra. Multiple TPs can be formed from one contaminant in biota when a molecule exhibits different sites for enzymatic attack or when one initial transformation enables consecutive enzymatic processing, including formation of phase-II metabolites.^{2,3}

Determination of all relevant TPs of a contaminant in biota is often hampered by the metabolome, a complex set of low-molecular-weight biogenic compounds that are coextracted with the transformation products. Although it is obvious that one should attempt to detect all TPs generated by the organism to establish the correct transformation pathway, this task becomes increasingly challenging when the number of TPs increases.

Received: May 5, 2015

Revised: September 1, 2015

Accepted: September 8, 2015

Published: September 8, 2015

TPs can be detected by two different approaches: (a) Suspect or target screening, which starts with the structure of the parent compound and first defines possible TPs that are then sought. (b) Nontarget screening, in which the study starts from the sample and interesting MS signals that may be related to TPs are sought.

Targets or suspects for the first approach, i.e., TPs that are sought by LC–HRMS, may be known from previous studies or derived from the molecular structure of the parent compound on the basis of transfer of knowledge or software prediction. When using the targeted approach, it seems essential to consider all possible transformation reactions in order to avoid missing TPs of relevance; excessively long lists of target compounds to search for do, however, increase the risk of false positive findings and may, therefore, be counterproductive.

The nontargeted approach always requires control samples, and it selects signals of interest from the data by assuming that they are only present in the sample containing the parent compound (and therefore also TPs) and not in the control. Considering that extracts of biota samples contain a large number of biogenic metabolites at much higher concentrations than the TPs, this selection of signals of interest in nontarget screening can become difficult.^{4,5} The analysis of samples taken repeatedly during a transformation process rather than solely at its end facilitates selection of interesting signals.⁶ Therefore, the combination of both target and nontarget screening seems advantageous.

Identification of TPs by HRMS relies on molecular formula identification on the basis of the exact mass of the molecular ion, its isotopic pattern and possible adduct ions, and on structure elucidation on the basis of the product ion spectrum. Software tools that help to compare a product ion spectrum with the suggested structure are available. However, the fragmentation processes can be complex, and the rearrangement of the carbon skeleton upon fragmentation is difficult to predict. In any case, the identification of a TP according to its mass spectrometric data remains tentative as long as no reference standard is available for comparison. Such standard materials are rarely available for TPs of environmental contaminants.

Electrochemistry (EC) coupled off-line or online to MS may support both detection and identification of TPs. This method has been used mainly to simulate transformation of drugs by phase-I and -II metabolism in higher organisms.^{7–9} Hydroxylation of activated aromatics, benzylic hydroxylation, N-dealkylation of amines, dealkylation of ethers and thioethers, S- and P-oxidation, oxidation of alcohols to aldehydes, and dehydration may be simulated by this method.⁸ Electrochemical transformation does not require the addition of any reagent, so the treated solutions can be analyzed directly without any need for cleanup that may lead to loss of TPs. However, EC oxidation is less site-specific than enzymatic oxidation, so a broader range of TPs may be formed. Thus, the set of TPs generated by EC may differ greatly from the set generated by higher organisms. EC as an analytical tool may be more suitable to simulate microbial transformations that involve enzymes other than those known to be found in higher organisms.

Biodegradation of organic substrates by white-rot fungi is often mediated by a variety of peroxidases, such as lignin peroxidases and manganese peroxidases.¹⁰ These enzymes, although acting in different ways depending on the specific enzyme, the substrate, and available cofactors, often form

intermediate radicals in their multistep electron transfer, as outlined in detail by Dashtban et al.¹¹ In terms of the variability and complexity of oxidation processes, this appears comparable to what is known for electrochemical oxidation. Also, multistep electron transfer at the electrode surface⁸ and oxidation by (hydroxy-) radicals in solution or bound to the electrode surface at pH <9 may occur.^{9,12}

Therefore, in this study we explored the potential of EC to support detection and identification of TPs in screening approaches using LC–HRMS. Transformation by the white-rot fungus *Pleurotus ostreatus*¹³ was studied, and the highly persistent pharmaceutical compound carbamazepine (CBZ) was chosen as the parent compound. CBZ is considered a marker of anthropogenic input into surface and groundwater.¹⁴ CBZ is a well-studied compound^{15–21} with numerous TPs already known, and some of these are commercially available. It is ideally suited to show how the use of electrochemistry supports the identification of TPs in complex mixtures.

■ EXPERIMENTAL SECTION

Chemicals. Acetonitrile, ammonium acetate, and acetic acid (all ULC/MS-grade) were from Biosolve (Valkenswaard, Netherlands). Ozonated CBZ samples in different proportions (1:1 and 1:4.5) stabilized with *t*-BuOH were a gift from Uwe Hübner (TU Berlin). CBZ, CBZ 10,11-epoxide, and 9-carboxylic acid acridine were purchased from Sigma-Aldrich (Munich, Germany), *cis*-10,11-dihydroxy-10,11-dihydrocarbamazepine (*cis*-diOH-CBZ), *rac trans*-10,11-dihydro-10,11-dihydroxy carbamazepine (*trans*-diOH-CBZ), and acridone were obtained from Biozol (Eching, Germany).

UPLC-Q-TOF-MS Analysis. The analysis was carried out on an ACQUITY UPLC system connected to a Synapt G2S equipped with an electrospray ionization source (Waters Corp., Milford, USA). A 10 μ L aliquot of each sample was injected into the column. UPLC separation was achieved using an ACQUITY UPLC BEH C18 column (100 \times 2.1 mm², 1.7 μ m) at a flow rate of 0.45 mL min⁻¹ with the column temperature was set to 45 °C. The mobile phase consisted of (B) ACN (0.01 M NH₄OAc, pH 5) and (A) 0.01 M NH₄OAc, pH 5. The following gradient was applied: 0–12.25 min, 2–99% B; 12.25–13.00 min, 99% B; 13.00–13.01 min, 99–2% B; and 13.01–14.00 min, 2% B. Ionization source conditions were as follows: capillary voltage of 0.7 kV, source temperature 140 °C, and desolvation temperature 550 °C. The sampling cone voltage was set to 35 V, and the source offset was set at 50 V. Nitrogen and argon were used as cone and collision gases, respectively. The desolvation gas flow was 950 L h⁻¹.

MS data were collected from *m/z* 50–1200 in negative and positive continuum mode with a 0.15 s scan time. To ensure accuracy during MS analysis, leucine enkephalin was infused via the reference probe as the lockspray, and a two-point calibration was applied. Two sets of data were collected in parallel using MS^E acquisition. One data set contained low-collision-energy data (4 eV, MS, effectively the accurate mass of precursors) and the second data set elevated-collision-energy data (15–35 eV, MS^E, all of the fragments).

Culture Conditions and Extraction. *P. ostreatus* strain PC9 was used in this study. Culture conditions are detailed in Golan-Rozen et al.¹³ Briefly, solid-state fermentation was conducted in 100 mL Erlenmeyer flasks using 2 g of chopped (<5 mm) cotton stalks as the substrate. Cotton stalks were moistened with 4 mL of ultrapure water and autoclaved. Then, 4 mL of aqueous CBZ solution was added to the cotton stalks

to a final amount of 0.22 μmol (0.05 mg) per flask. The inoculum was one disk (5 mm diameter) of mycelium obtained from the edge of a young colony grown on solid glucose-peptone medium. Cultures were incubated at 28 °C in the dark for 60 days. Two types of controls were used: inoculated but without substrate and noninoculated with substrate. Once a week, three flasks were harvested and stored at -80 °C. All samples were lyophilized and weighed in 50 mL conical tubes. Then, 30 mL of MeOH was added to each tube. Samples were sonicated using an ultrasonic probe (20 kHz), agitated for 30 min (200 rpm), and centrifuged (~ 4000 g, 15 min). Supernatants were filtered through a 0.2 μm Teflon filter and stored at -80 °C until analysis. Extract (3 mL) was dried under a gentle N_2 stream, reconstituted in 400 μL of MeOH, and vortexed rigorously. Samples were diluted 1:1 (v/v) with ultrapure water, mixed, and centrifuged (10 min) to remove insoluble material. Control samples were treated in the same way.

Electrochemistry. EC oxidation was carried out using a commercially available EC ReactorCell (Antec, The Netherlands) equipped with a boron-doped diamond working electrode (BDD, Magic Diamond, Antec), a HyREF (Pd/ H_2) reference electrode, and an auxiliary electrode made of carbon-loaded PTFE (not isolated from the working electrode). An infusion pump was used to oxidize in flow-through mode ($10 \mu\text{L min}^{-1}$) a 40 μM CBZ (approximately 10 $\mu\text{g/mL}$) solution in 75% NH_4Ac (0.02 M NH_4OAc , pH 7) and 25% MeOH (v/v) at various potentials (0, 0.5, 1.0, 1.5, 2, and 2.5 V). The potentials were applied using ROXY potentiostat (Antec) controlled by Dialogue software (Antec). The same experiment was carried out with a 40 μM acridine solution to verify the transformation to acridone.

Data Processing. Target screening in data of fungal treatment was done as follows: Continuum raw MS data were processed using Unifi software (Waters). Automatic 3D Peak Processing settings were used, and the target-match tolerance was set to 5 ppm. Adduct protonation, sodium, potassium, and ammonium were selected, and a lock mass (leucine enkephalin, m/z 556.2771) correction was carried out. The chromatogram of the EC treatment was set as a reference, and using a filter method, only candidates and expected transformations were shown (match type: common). These candidates were verified by two other replicates of the sample. By sorting according to retention time, we ensured that no fragments were selected as separate TPs. For expected TPs, additional filters were a δ mass below 5 ppm, isotope-match intensity RMS percentage above 20%, and isotope-match M_z RMS 5 ppm. A common search for fragment ions was carried out to detect further candidates.

Nontarget screening was done according to a previously established procedure²² for the fungal generated samples. Briefly, centroid raw MS data were processed using MarkerLynx application manager for MassLynx 4.1 software (Waters). The intensity of each ion was normalized with respect to the total ion count to generate a data matrix that consists of retention time, m/z value, and normalized peak area. The unsupervised segregation of control and exposed fungal samples was checked by principal component analysis (PCA) using pareto-scaled data. The loading plot of the supervised partial least-squares discriminant analysis (PLS-DA) and orthogonal projection to latent structures (OPLS) enabled the identification of analytes responsible for the separation of control and exposed samples. These analytes were extracted as

results. The procedure was applied for low- and high-collision-energy data to align precursor and fragments.

RESULTS AND DISCUSSION

Products Formed by Electrochemical Oxidation of CBZ. To generate TPs as possible analytical targets for the screening for TPs formed during degradation of CBZ by *P. ostreatus*, a CBZ solution was oxidized while flowing through an EC cell at different voltages (0.5, 1.0, 1.5, 2.0, and 2.5 V), and collected for LC–HRMS analysis. At 1.5 V, the initial CBZ concentration began to decrease, and several new signals appeared in the LC–MS chromatogram. As the voltage increased, the TP pattern changed (Figure 1). However, no

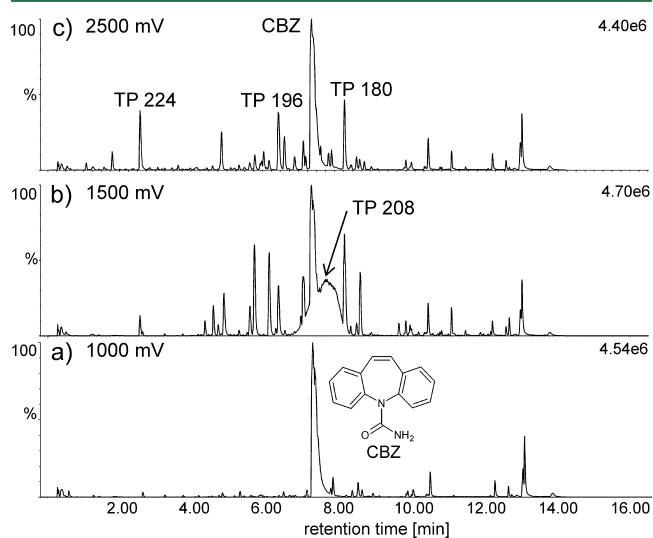


Figure 1. Base peak chromatograms of electrochemically treated CBZ analyzed by LC–HRMS. (a) 1000 mV, (b) 1500 mV, and (c) 2500 mV.

clear sequence of TP formation could be established by the variation of potentials or the residence time (by changing the flow rate) in the EC cell. This might have been for thermodynamic reasons, e.g., a certain redox potential has to be exceeded for the formation of a certain product, or for kinetic reasons, e.g., certain processes of a set of competing reactions may be faster than others at different potentials.

Because no reagents were added in this oxidation procedure, each novel signal detected by LC–HRMS in the CBZ solution upon EC oxidation indicated a electrochemically derived TP (Figure 1). The LC–HRMS data generated by this approach were screened for MS signals with a software routine (within Unifi) using predefined criteria for mass accuracy and possible elemental compositions. For a potential of 1.5 V, a total of 105 signals fulfilled the criteria and were listed with their chromatographic retention time, exact mass, and isotopic pattern of the molecular ion, molecular formula, and the product ion spectrum. This list was manually reduced to 68 signals by deleting obvious in-source fragments and signals that were repeatedly stored because of poor shape of the chromatographic peak.

Because EC treatment was carried out to generate analytical targets in the screening for fungal TPs, it was not necessary to process further all signals and to identify all TPs. Only signals that were also present in the fungus-treated CBZ extract under the same analytical conditions were of interest. Comparison of

Table 1. Lists of Transformation Products (TPs) of Carbamazepine (CBZ) Detected and Identified in CBZ Exposed to the Fungus *Pleurotus ostreatus* by Comparison with the Electrochemical Oxidation Experiment^a

name	t_R (min)	m/z	predicted formula	fragments (m/z)	predicted formula (fragments)	refs	verified by
TPs Determined by Target Screening for Molecular Ions							
TP 224 9-carboxylic acid-acridine	2.36	224.0712	$C_{14}H_{10}NO_2$ (-3.1)	196.0758 180.0805 167.0735	$C_{13}H_{10}NO$ (2.0) $C_{13}H_{10}N$ (4.4) $C_{12}H_9N$ (2.4)	3	standard
TP 253a <i>cis</i> -dihydro-dihydroxy-carbamazepine	3.81	293.0170	$C_{15}H_{14}N_2O_3Na$ (-1.4)	210.0928 180.0817 265.0620	$C_{14}H_{12}NO$ (4.3) $C_{13}H_{10}N$ (2.2) $C_{15}H_9N_2O_3$ (1.1)	23	standard
TP 283 1-(2-benzoic acid)-(1H,3H)-quinazoline-2,4-dione (BaQD)	4.69	283.0725	$C_{15}H_{11}N_2O_4$ (-2.1)	240.0662 196.0762 166.0656	$C_{14}H_{10}NO_3$ (0.4) $C_{13}H_{10}NO$ (0) $C_{12}H_8N$ (0.6)	18	ozone sample
TP 253b <i>trans</i> -dihydro-dihydroxy-carbamazepine	5.47	253.0975 293.0209	$C_{15}H_{13}N_2O_2$ (0.8) $C_{15}H_{14}N_2O_3Na$ (-0.3)	210.0917 180.0814 182.0963	$C_{14}H_{12}NO$ (1.4) $C_{13}H_{10}N$ (0.6) $C_{13}H_{12}N$ (3.8)	24	standard
TP 253c carbamazepine epoxide	5.87	275.0803 253.0983	$C_{15}H_{12}N_2O_2Na$ (0.7) $C_{15}H_{13}N_2O_2$ (-1.6)	236.0715 210.0921 180.0815 167.0737	$C_{15}H_{10}NO_2$ (1.3) $C_{14}H_{12}NO$ (1.0) $C_{13}H_{10}N$ (1.1) $C_{12}H_9N$ (1.2)	24, 25	standard
TP 196 acridone	6.1	196.0762	$C_{13}H_{10}NO$ (-4.6)	180.0813 167.0739 250.0509	$C_{13}H_{10}N$ (0) $C_{12}H_9N$ (2.4) $C_{15}H_8NO_3$ (2)	3, 20, 19	standard
TP 267b 4-formyl-9-oxoacridine-10(9H)-carboxamide	6.24	267.0771	$C_{15}H_{11}N_2O_3$ (-0.4)	224.0710 196.0769	$C_{14}H_{10}NO_2$ (2.1) $C_{13}H_{10}NO$ (4.1)	17	proposed
TP 267c 10-methoxy-carbamazepine	6.88	267.1132	$C_{16}H_{15}N_2O_2$ (-0.7)	224.1082	$C_{15}H_{14}NO$ (3.1)	this study	proposed
TP 208 9-acridine-carboxaldehyde (hemiacetal)	7.59	240.1025	$C_{15}H_{14}NO_2$ (-1.2)	208.0762 180.0813	$C_{14}H_{10}NO$ (1.0) $C_{13}H_{10}N$ (0.6)	20, 29	proposed
TP 180 acridine	8.03	180.0815	$C_{13}H_{10}N$ (-1.1)	167.0735	$C_{12}H_9N$ (2.4)	20, 19	standard
TPs Determined by Screening for Product Ions							
TP 251	5.57	251.0821	$C_{15}H_{11}N_2O_2$ (0)	208.0771 180.0805 224.0712	$C_{14}H_{10}NO$ (4.3) $C_{13}H_{10}N$ (4.4) $C_{14}H_{10}NO_2$ (0)	21	proposed
TP 267a 1-(2-benzaldehyde)-(1H,3H)-quinazoline-2,4-dione (BQD)	5.6	267.0771	$C_{15}H_{10}N_2O_3$ (-0.4)	196.0762 167.0737 254.0820	$C_{13}H_{10}NO$ (0) $C_{12}H_9N$ (1.2) $C_{15}H_{12}NO_3$ (2.1)	18	ozone sample
TP 272 10,11-dihydroxy-10,11-dihydro-5H-dibenzo[b,f]azepine-5-carboxylic acid	8.21	272.0932	$C_{15}H_{14}NO_4$ (-3.3)	222.0552 196.0769 254.0820	$C_{14}H_8NO_2$ (1.4) $C_{13}H_{10}NO$ (3.6) $C_{15}H_{12}NO_3$ (1.2)	this study	proposed
TP 286 10-hydroxy-11-methoxy-10,11-dihydro-5H-dibenzo[b,f]azepine-5-carboxylic acid	10.15	286.1085	$C_{16}H_{16}NO_4$ (-2.1)	240.0661 222.0550 196.0772	$C_{14}H_{10}NO_3$ (0) $C_{14}H_8NO_2$ (1.4) $C_{13}H_9NO$ (4.1)	this study	proposed
TP Determined by Nontarget Screening							
TP 281 methyl 2-(2-oxoquinazolin-1(2H)-yl)benzoate	7.24	281.0938	$C_{16}H_{12}N_2O_3$ (-4.3)	249.0674	$C_{15}H_9N_2O_2$ (4.0)	this study	proposed

^aFor TP structures, please refer to Figure 4.

the two treatments and selection of MS signals occurring in both were carried out using the software Unifi. In this way, 10 signals were selected as possible TPs (Table 1), and their MS data were used for tentative identification. For TPs of low intensity in the LC–HRMS analysis, the EC oxidation could be easily repeated at elevated concentrations to obtain clear product ion spectra. The fragments of the identified TPs were collected, structures were proposed, and the common fragment ions (Table S1) were used to detect further TPs in the fungal samples (see below). The thorough study of the fragment ions

also supported the identification of substructures of TPs. In this way, EC combined with LC–HRMS supported both detection of TPs generated during degradation of CBZ by *P. ostreatus*¹³ and their identification, as detailed below.

The dominant signal in the base peak chromatogram of the EC-derived sample at 1.5 V was a broad peak ($t_R = 7.59$ min, TP 240) that disappears at higher voltages (Figure 1b). It was also detected in the fungal extract, albeit at lower intensity. This signal, with a molecular cation of m/z 240.1025 ($C_{15}H_{14}NO_2$), exhibited fragment ions of m/z 208.0762 ($C_{14}H_{10}NO$) and m/z

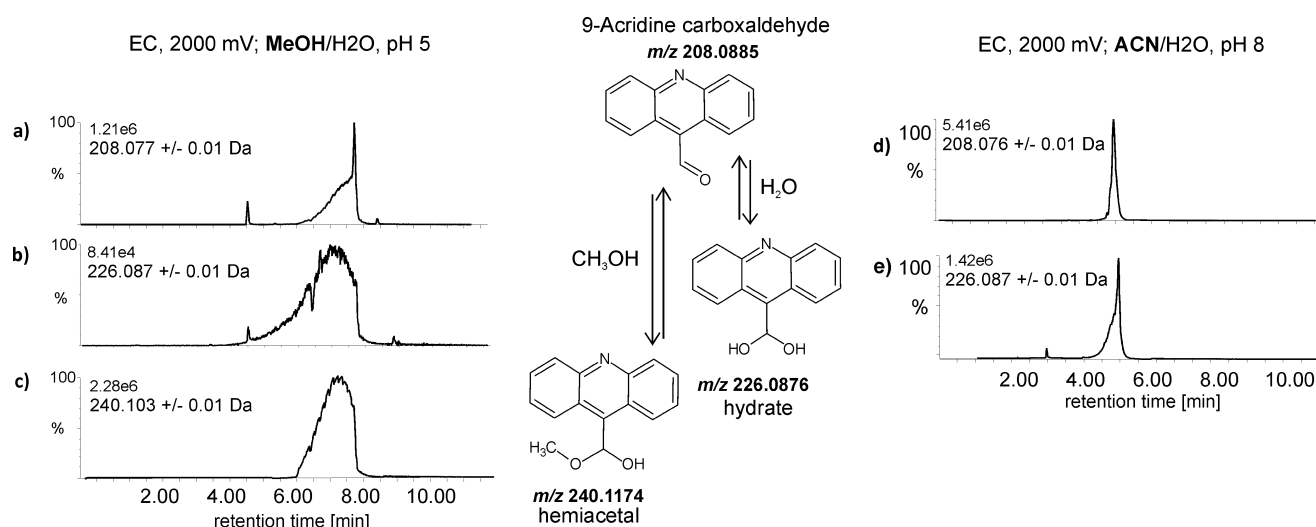


Figure 2. Extracted ion chromatograms of TP 240 and its putative hydrate and hemiacetal forms: (a–c) with water/MeOH eluent (pH 5) and (d and e) with water/ACN eluent (pH 8).

180.0813 ($C_{13}H_{10}N$). Both fragmentations (loss of CH_3OH and subsequent CO) suggested two optional structures of this TP: 9-acridine carboxaldehyde and (9,10)-keto-methoxyiminostilbene. Although the latter would be expected to elute as a narrow peak, 9-acridine carboxaldehyde may form a hydrate as well as a hemiacetal in the eluent (water and MeOH, pH 5). Indeed, the corresponding molecular ions coeluted with TP 240 (Figure 2a–c). The broad chromatographic peak suggests that the aldehyde equilibrates during chromatography with its hemiacetal (m/z 240.1174) and hydrate (m/z 226.0876) forms. In a repeated analysis under different conditions (pH 8, ACN), only the carboxaldehyde and the hydrate were determined (Figure 2d,e). The absence of the hemiacetal form is due to the replacement of MeOH in the eluent, and the smaller peak shape indicates faster equilibration between 9-acridine carboxaldehyde and its hydrate form during chromatography at pH 8 as compared to that at pH 5.¹⁵

Formation of isomers with the same molecular ion and often very similar fragment ions is a common feature in transformation studies and a source of erroneous identification by LC–MS. Therefore, it is essential to ensure separation of isomers by chromatography, and this often requires repeat analyses. However, extracts of biological samples are often limited in volume and do not allow repeated analyses under different analytical conditions. The EC oxidation of CBZ in the laboratory is easily repeated within a few minutes, enabling repeat analyses to optimize chromatographic separation (see below). Moreover, case-wise optimization of the chromatography may also be needed for successful target screening for TPs in the biological samples. As long as the targets are unknown, such optimization cannot be carried out. The combination of EC and LC–HRMS is also advantageous in this respect. Furthermore, repeated electrochemical oxidation of the parent compound may be used to generate sufficient material for a subsequent NMR analysis to confirm a proposed structure.

Another series of isomeric CBZ TPs occurred at m/z 267.077 ($C_{15}H_{11}N_2O_3$) (Figure S2). Two TPs of this formula have been identified as ozonation products of CBZ: BQD and BaQM.¹³ A third TP with a slightly longer retention time ($t_R = 6.24$ min) was determined upon EC oxidation. Its fragment cations m/z 250.051 ($C_{15}H_8NO_3$), m/z 224.071 ($C_{14}H_{10}NO_2$),

and m/z 196.077 ($C_{13}H_{10}NO$) indicate loss of NH_3 and a carbamoyl moiety ($CHNO$) as well as subsequent loss of CO , suggesting an aldehyde or keto group within the seven-membered ring of CBZ and the presence of an amino group. Two structural proposals were elaborated: 11-keto oxcarbamazepine and 4-formyl-9-oxoacridine-10(9H)-carboxamide. It was identified as the latter (TP 267b, Table 1) because of its comparatively broad peak; this compound may tautomerize into a cyclic form with different retention behavior during chromatography at acidic pH (Figure S3).

Another signal of very similar mass (m/z 267.113, $C_{16}H_{15}N_2O_2$) and only slightly longer retention time (6.88 min) was found in the EC sample as well as the fungal-treated sample (TP 267a, Table 1). Its small difference of 0.036 Da relative to the three TPs discussed above outlines the need for a MS with high mass-resolving power as well as high mass accuracy and precision.

Additional Target and Nontarget Screening. The targets or suspects in a list for screening purposes are usually obtained from previous studies that may be specific for the compound under study or originate from structurally related ones. CBZ is a very well-studied contaminant, and therefore much information on possible TPs is available.^{3,16–21} Correspondingly, 9 of the 10 TPs detected and identified by EC with LC–HRMS had been previously described (Table 1). This proves that EC oxidation is indeed feasible for the generation of relevant TPs of environmental contaminants by both biotic and abiotic processes. Six of these CBZ TPs are commercially available, but this is generally not the case. If TP standards are not available, then the use of EC with LC–HRMS is attractive because such experiments provide the full set of MS and chromatographic data with the very same analytical system that will subsequently be used for the target screening. In the case of structural isomer formation, data from previous studies are often insufficient for correct identification, as already noted.

In the case that literature does not provide clear information on expected TPs, the definition of analytical targets may be supported by software prediction of potential TPs, e.g., by UM-BBD/EAWAG-BBD.⁵ However, in the case of CBZ, this program does not provide any useful prediction of TPs. None of the TPs formed in these experiments, i.e., the ring-opening

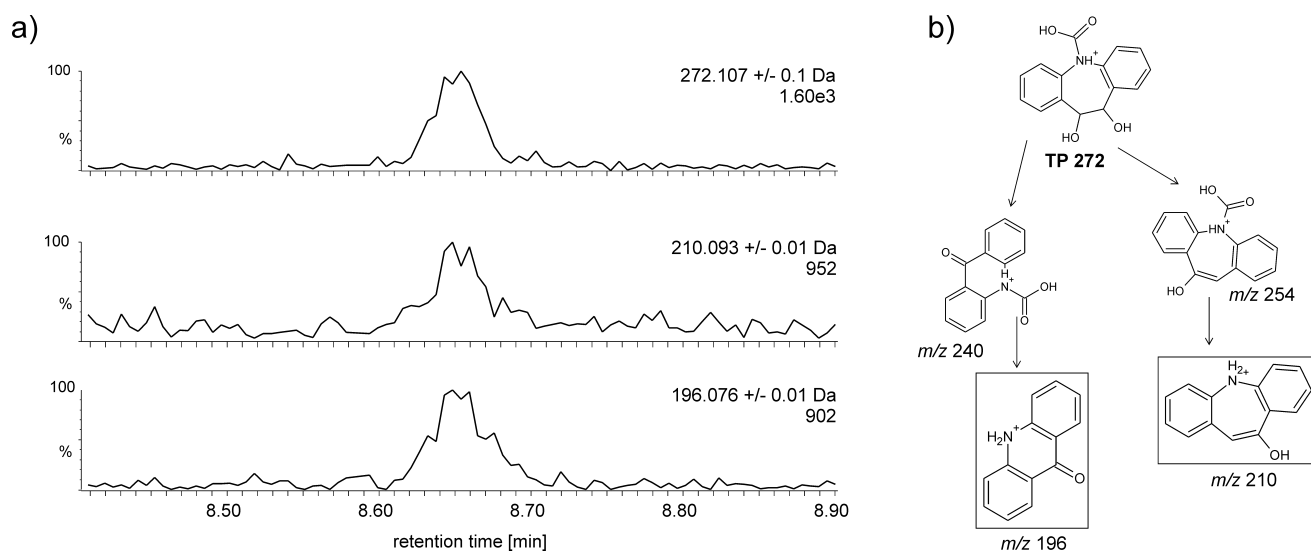


Figure 3. (a) Extracted ion chromatograms of TP 272 and the common fragments m/z 196 and 210 used for identification. (b) m/z 254 and 240 were assigned as intermediate fragments and were used for structure elucidation.

products or the acridine derivatives, were predicted by the software.

Not only can the molecular ions of TPs generated by EC treatment be used for target screening, but also can their fragment ions be employed. By screening the data set of the fungus-treated CBZ sample for these 18 fragment ions, another 4 CBZ TPs were determined (Table 1), two of which (TP 286 and TP 272, Table 1) had never been reported for either microbial or chemical treatment of CBZ. Structure proposals were elaborated on the basis of the exact masses of the molecular cations and the fragment ions.

The common fragments m/z 196.0758 ($C_{13}H_{10}NO$) and m/z 210.0928 ($C_{14}H_{12}NO$) allowed detection of TP 272 (Figure 3). This illustrates a case in which different TPs exhibit some identical fragment ions. The uncommon fragment ions m/z 254.0820 ($C_{15}H_{12}NO_3$) and m/z 240.066 ($C_{14}H_{10}NO_3$) supported the structure elucidation of these novel TPs (Table 1). TP 272 and TP 286 may originate from the well-known diOH-CBZ by hydrolysis of its carbamoyl moiety to a carboxylic acid. For the parent CBZ, hydrolysis of the carbamoyl moiety is not favored because of resonance stabilization. Because these two TP 272 and TP 286 have never been reported in literature, this hydrolysis appears to be a very specific transformation by *P. ostreatus*.

The third TP observed by common fragment screening was TP 251, with a molecular ion of m/z 251.098 ($C_{15}H_{10}N_2O_2$, t_R = 6.0 min), which was present only in the fungal sample. This TP has the same molecular formula but a different retention time than BQM (t_R = 6.3 min), which was formed by EC and previously found upon ozonation.¹⁴ However, TP 251 also formed some fragment ions identical to those formed by BQM, namely m/z 180.080 ($C_{13}H_{10}N$) and m/z 208.077 (Table 1). On the basis of the MS data, a four-ringed system is proposed for TP 251 (Figure S4). It could be formed via 2-hydroxy-CBZ and iminoquinone, which would rearrange into a fully conjugated structure as previously proposed by Martínez et al.²¹

For well-studied parent compounds such as CBZ, such a search for undetected TPs can be carried out using literature data on fragment ions. Indeed, for CBZ the use of scientific papers^{16–21} or open-source mass spectra libraries, e.g., mzCloud, MassBank, and METLIN, would have resulted in a

similar list of TPs (Table S1). For new compounds, however, for which TPs and their mass spectrometric fragmentation are unknown, EC combined with LC-HRMS is a powerful source for such data on fragment ions to search for in the real samples.

Finally, a nontarget screening for CBZ TPs was carried out in fungus-treated CBZ extracts and compared to blank fungal extracts as a control. This approach resulted in the determination of one additional TP (TP 281, Table 1) that was not reported before as a TP of CBZ formed either by a biotic or abiotic process. Although the EC approach combined with target screening led to the determination of most fungal TPs of CBZ, it did not detect all its TPs. Therefore, the complementary use of nontarget screening remains useful. Surprisingly, no phase-II metabolites were detected by the nontarget screening.

Practical experience with nontarget screening for TPs in biota shows that care must be taken to avoid false findings from the metabolome of the organisms because these biogenic metabolites may change during the development of organisms or culture growth. Moreover, the exposure of an organism to the study compound may affect its metabolome so that even signals becoming obvious from the analysis of a time series of the exposure/degradation experiment may be biogenic metabolites rather than TPs of the study compound.

CBZ, similar to most biogenic molecules, consists of only carbon, hydrogen, oxygen, and nitrogen. Therefore, CBZ and its TPs exhibit mass defects that are in the range occupied by the ions of the fungal metabolome. This hampers the detection of TPs, and very high mass-resolving power as well as high mass accuracy and precision are thus required in nontarget screening to distinguish CBZ TPs from the fungal metabolome.²⁶

Comparison of CBZ TPs Formed by EC and *P. ostreatus*. A total of 10 TPs were found by target screening on the basis of the EC experiment. Another four TPs were found by screening for fragment ions, and eventually, one more was found by nontarget screening in the fungal extract (Table 1). By providing access to 14 of 15 TPs, the use of EC effectively supports the identification of TPs. Other oxidation experiments may be carried out in the laboratory to generate possible biogenic TPs. However, in the case of CBZ, neither

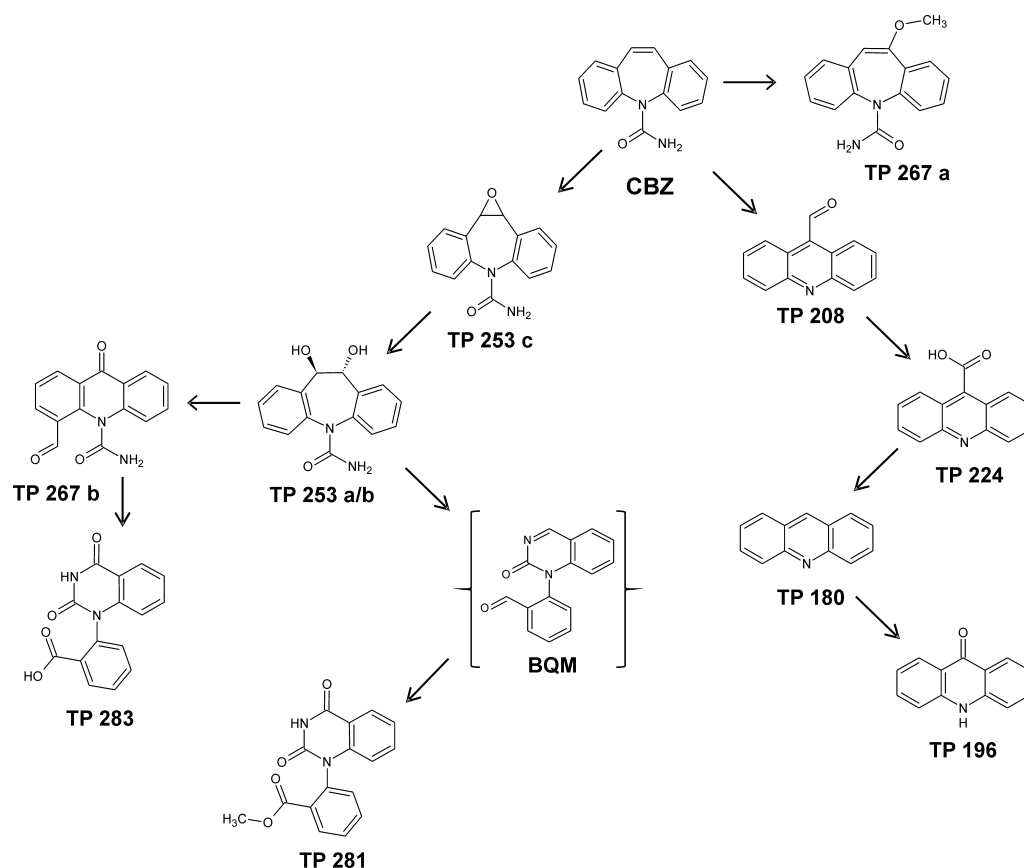


Figure 4. Structures of the identified transformation products of CBZ formed by EC and by fungal (*P. ostreatus*) treatment. Left, diOH-CBZ pathway, and right, acridine pathway.

photocatalysis²¹ nor ozone^{16,18} nor ferrate¹⁷ generated all 14 fungal TPs found after EC treatment.

The 15 TPs can be arranged into two major CBZ-degradation pathways: the acridine pathway and the diOH-CBZ pathway (Figure 4). Comparing the relative intensities of the different CBZ TPs formed by EC and fungal treatment (Figure S1), it appears that EC prefers the acridine pathway, whereas the fungal treatment favors the diOH-CBZ pathway.¹³ This may well reflect the different mechanisms of oxidation, i.e., enzymatic oxidation by the fungus and oxidation at the surface of the diamond electrode in EC. Aside from this general pattern, a few more detailed differences are of interest.

The acridine pathway, which is dominant in the EC treatment, has been observed during photodegradation of CBZ and during its oxidation by chlorine dioxide.^{19,26} In EC samples, we found comparable signal intensities for all four members of this series: acridine carboxaldehyde (TP 208), acridine-9-carboxylic acid (TP 224), acridine (TP 180), and acridone (TP 196). These four TPs probably originate from the initial oxidation of the central double bond of CBZ and abstraction of the carbamoyl moiety. Electron-withdrawing groups at the fourth position to the *N*-alkyl group facilitate dealkylation with Fenton reagent,²⁷ and other radical mechanisms are likely to also be supported.

Imide may occur as an intermediate, but it may be too reactive to allow its detection.²⁸ Ring contraction and rearrangement would lead to acridine carboxaldehyde, the oxidation of which leads to acridine-9-carboxylic acid. Decarboxylation leads to acridine, which is converted to acridone by hydroxylation and oxidation (Figure 4).

Transformation pathways are best elucidated by using intermediates as educts and following their transformation.¹³ Although in biological studies this requires a complete set of new exposure experiments that may last for days to weeks, in EC this is done within minutes. Such an experiment was carried out here to confirm the formation of acridone from acridine (Figure S5).

Differences were also found along the diOH-CBZ pathway. For the fungal, enzyme-driven hydrolysis of 10,11-epoxy carbamazepine (EP-CBZ, TP 253c), *trans*-diOH-CBZ (TP 253b) was the only diOH-CBZ isomer expected.¹³ However, the *cis*-isomer (TP 253a) was also detected, albeit at approximately one-quarter of the intensity of the *trans* isomer. In contrast, upon EC transformation, both *cis* and *trans* isomers were formed to the same extent. This supports the assumption that in EC the hydrolysis of EP-CBZ occurs in two steps with the formation of a carbo-cation intermediate that may be stabilized by the neighboring aryl groups.²⁹

Further differences were observed in later stages of the diOH-CBZ pathway: stepwise oxidation of diOH-CBZ proceeded via BQM (TP 251) and BQD (TP 267a) to the comparatively stable BaQD (TP 283, Figure 4). This process was also found upon ozonation of CBZ,¹⁸ as well as by wet oxidation by KMnO₄ or ferrate.¹⁷ In the fungal system, however, BQM (TP 251) was not detected, but rather a methylated variant and the two subsequent products were found (Figure 4). In the EC treatment, BQM (TP 251) was detected. However, the next oxidation product, BQD (TP 267c), was missing, whereas the stable BaQD was present. BQD (TP 267c) is either very reactive toward EC oxidation

and is therefore rapidly transformed or not generated at all, in which case BaQD (TP 283) is directly formed from BQM (TP 251). TP 267b is a newly identified TP that occurred in both EC and fungal treatments. This TP opens a novel route to the stable BaQD (TP 283) (Figure 4).

Future Application of EC with LC–HRMS. In the case of the well-studied compound CBZ, generation of TPs by EC provided a useful tool for targeted screening of TPs generated by *P. ostreatus* via LC–HRMS because it supported TP detection and identification.¹³ This approach is also promising for the study of other compounds and biological transformation processes as well as oxidative technical treatment processes, namely, when radicals are involved. EC can also be applied under reducing conditions. However, the suitability of EC under reducing conditions to simulate reductive microbial degradation needs to be proven.

Online coupling of EC with LC–HRMS allows establishment of an automated system that can analyze the transformation of a larger number of compounds without manual processing. In this way, the transformation of a larger number of compounds can be studied, and the MS data of the TPs can be fed into a database (in-house or web-based, e.g., MassBank) suited for a broader search for TPs of contaminants in the environment or biota. Knowledge on the reactivity and transformation of chemicals will support our understanding of their fate in biological and technical systems.

■ ASSOCIATED CONTENT

Supporting Information

The Supporting Information is available free of charge on the ACS Publications website at DOI: 10.1021/acs.est.5b02229.

Typical fragment cations of CBZ and its TPs and proposed structures (Table S1), relative intensity of the TPs in EC (1.5 V) and fungal treatments (Figure S1), extracted ion chromatogram of *m/z* 267.077 and possible structures for the fungus- and EC-treated samples (Figure S2), the keto-amino-TP with its tautomeric forms (Figure S3), proposed pathways for the formation of TP 251 (Figure S4), and formation of acridone from acridine by EC treatment (Figure S5). (PDF)

■ AUTHOR INFORMATION

Corresponding Author

*Tel.: +49 (0341) 235 1261. Fax: +49 (0341) 235 450822.

Notes

The authors declare no competing financial interest.

■ ACKNOWLEDGMENTS

We thank Coretta Bauer for extensive technical assistance. This work was funded in part by the Deutsche Forschungsgemeinschaft (DFG, Bonn, Germany) through the project PECtake (Re1290/7-1). We are grateful to four anonymous reviewers for their helpful comments.

■ REFERENCES

- (1) Bletsou, A. A.; Jeon, J.; Hollender, J.; Archontaki, E.; Thomaidis, N. S. Targeted and non-targeted liquid chromatography-mass spectrometric workflows for identification of transformation products of emerging pollutants in the aquatic environment. *TrAC, Trends Anal. Chem.* **2015**, *66*, 32–44.
- (2) Yang, Y. Y.; Pereyra, L. P.; Young, R. B.; Reardon, K. F.; Borch, T. Testosterone-mineralizing culture enriched from swine manure:

characterization of degradation pathways and microbial community composition. *Environ. Sci. Technol.* **2011**, *45* (16), 6879–86.

- (3) Kaiser, E.; Prasse, C.; Wagner, M.; Broder, K.; Ternes, T. A. Transformation of oxcarbazepine and human metabolites of carbamazepine and oxcarbazepine in wastewater treatment and sand filters. *Environ. Sci. Technol.* **2014**, *48* (17), 10208–10216.

- (4) Hernández, F.; Ibáñez, M.; Bade, R.; Bijlsma, L.; Sancho, J. V. Investigation of pharmaceuticals and illicit drugs in waters by liquid chromatography-high-resolution mass spectrometry. *TrAC, Trends Anal. Chem.* **2014**, *63*, 140–157.

- (5) Kern, S.; Fenner, K.; Singer, H. P.; Schwarzenbach, R. P.; Hollender, J. Identification of Transformation Products of Organic Contaminants in Natural Waters by Computer-Aided Prediction and High-Resolution Mass Spectrometry. *Environ. Sci. Technol.* **2009**, *43* (18), 7039–7046.

- (6) Helbling, D. E.; Hollender, J.; Kohler, H.-P. E.; Singer, H.; Fenner, K. High-Throughput Identification of Microbial Transformation Products of Organic Micropollutants. *Environ. Sci. Technol.* **2010**, *44* (17), 6621–6627.

- (7) Lohmann, W.; Baumann, A.; Karst, U. Electrochemistry and LC-MS for Metabolite Generation and Identification: Tools, Technologies and Trends. *LCGC North Am.* **2010**, *28* (6), 470–476.

- (8) Jurva, U.; Wikström, H. V.; Weidolf, L.; Bruins, A. P. Comparison between electrochemistry/mass spectrometry and cytochrome P450 catalyzed oxidation reactions. *Rapid Commun. Mass Spectrom.* **2003**, *17* (8), 800–810.

- (9) Faber, H.; Vogel, M.; Karst, U. Electrochemistry/mass spectrometry as a tool in metabolism studies—a review. *Anal. Chim. Acta* **2014**, *834*, 9–21.

- (10) Grinhut, T.; Hertkorn, N.; Schmitt-Kopplin, P.; Hadar, Y.; Chen, Y. Mechanisms of humic acids degradation by white rot fungi explored using 1H NMR spectroscopy and FTICR mass spectrometry. *Environ. Sci. Technol.* **2011**, *45* (7), 2748–54.

- (11) Dashtban, M.; Schraft, H.; Syed, T. A.; Qin, W. Fungal biodegradation and enzymatic modification of lignin. *Int. J. Biochem. Mol. Biol.* **2010**, *1* (1), 36–5011.

- (12) Enache, T. A.; Chiorcea-Paquim, A.-M.; Fatibello-Filho, O.; Oliveira-Brett, A. M. Hydroxyl radicals electrochemically generated in situ on a boron-doped diamond electrode. *Electrochem. Commun.* **2009**, *11* (7), 1342–1345.

- (13) Golan-Rozen, N.; Seiwert, B.; Riemenschneider, C.; Reemtsma, T.; Chefetz, B.; Hadar, Y. Transformation Pathways of the Recalcitrant Pharmaceutical Compound Carbamazepine by the White-rot Fungus *Pleurotus ostreatus*: Effects of growth conditions. *Environ. Sci. Technol.* **2015**, DOI: 10.1021/acs.est.5b02222.

- (14) Reemtsma, T.; Weiss, S.; Mueller, J.; Petrovic, M.; Gonzalez, S.; Barcelo, D.; Ventura, F.; Knepper, T. Polar pollutant entry into the water cycle by municipal wastewater: a European perspective. *Environ. Sci. Technol.* **2006**, *40* (17), 5451–5458.

- (15) McClelland, R. A.; Sukhai, P.; Engell, K. M.; Sorensen, P. E. Hydration Equilibria of 9-Acridinecarboxaldehyde. *Can. J. Chem.* **1994**, *72* (11), 2333–2338.

- (16) Hubner, U.; Seiwert, B.; Reemtsma, T.; Jekel, M. Ozonation products of carbamazepine and their removal from secondary effluents by soil aquifer treatment - Indications from column experiments. *Water Res.* **2014**, *49*, 34–43.

- (17) Hu, L.; Martin, H. M.; Arce-Bulted, O.; Sugihara, M. N.; Keating, K. A.; Strathmann, T. J. Oxidation of Carbamazepine by Mn(VII) and Fe(VI): Reaction Kinetics and Mechanism. *Environ. Sci. Technol.* **2009**, *43* (2), 509–515.

- (18) McDowell, D. C.; Huber, M. M.; Wagner, M.; Von Gunten, U.; Ternes, T. A. Ozonation of carbamazepine in drinking water: Identification and kinetic study of major oxidation products. *Environ. Sci. Technol.* **2005**, *39* (20), 8014–8022.

- (19) Kosjek, T.; Andersen, H. R.; Kompere, B.; Ledin, A.; Heath, E. Fate of Carbamazepine during Water Treatment. *Environ. Sci. Technol.* **2009**, *43* (16), 6256–6261.

(20) Fürst, S. M.; Uetrecht, J. P. Carbamazepine Metabolism to a reactive intermediate by the myeloperoxidase system of activated neutrophils. *Biochem. Pharmacol.* **1993**, *45* (6), 1267–1275.

(21) Martínez, C.; Canle L., M.; Fernández, M. I.; Santaballa, J. A.; Faria, J. Kinetics and mechanism of aqueous degradation of carbamazepine by heterogeneous photocatalysis using nanocrystalline TiO₂, ZnO and multi-walled carbon nanotubes–anatase composites. *Appl. Catal., B* **2011**, *102* (3–4), 563–571.

(22) Macherius, A.; Seiwert, B.; Schroder, P.; Huber, C.; Lorenz, W.; Reemtsma, T. Identification of Plant Metabolites of Environmental Contaminants by UPLC-QToF-MS: The in Vitro Metabolism of Triclosan in Horseradish. *J. Agric. Food Chem.* **2014**, *62* (5), 1001–1009.

(23) De Laurentiis, E.; Chiron, S.; Kouras-Hadef, S.; Richard, C.; Minella, M.; Maurino, V.; Minero, C.; Vione, D. Photochemical Fate of Carbamazepine in Surface Freshwaters: Laboratory Measures and Modeling. *Environ. Sci. Technol.* **2012**, *46*, 8164–8173.

(24) Jelić, A.; Cruz-Morató, C.; Marco-Urrea, E.; Sarrà, M.; Pérez, S.; Vicent, T.; Petrović, M.; Barceló, D. Degradation of carbamazepine by *Trametes versicolor* in an air pulsed fluidized bed bioreactor and identification of intermediates. *Water Res.* **2012**, *46*, 955–964.

(25) Kang, P.; Liao, M.; Wester, M. R.; Leeder, J. S.; Pearce, R. E.; Correia, M. A. CYP3A4-Mediated Carbamazepine (CBZ) Metabolism: Formation of a Covalent CBZ-CYP3A4 Adduct and Alteration of the Enzyme Kinetic Profile. *Drug Metab. Dispos.* **2007**, *36*, 490.

(26) Krauss, M.; Singer, H.; Hollender, J. LC-high resolution MS in environmental analysis: from target screening to the identification of unknowns. *Anal. Bioanal. Chem.* **2010**, *397* (3), 943–951.

(27) Doll, T. E.; Frimmel, F. H. Removal of selected persistent organic pollutants by heterogeneous photocatalysis in water. *Catal. Today* **2005**, *101* (3–4), 195–202.

(28) Zbaida, S.; Gilhar, D.; Silman-Greenspan, J. Replacing the mixed function oxidase N-demethylation by hydrogen peroxide and either hemoglobin or ferrous sulfate. *Pharm. Res.* **1984**, *1* (6), 277–279.

(29) Kawashima, K.; ISHIGURO, T. On the Reactions of Dibenz[b,f]oxireno[d]azepine Derivatives. *Chem. Pharm. Bull.* **1978**, *26* (3), 951–955.